FISH & CHIPS: Four Electrode Conductivity / Salinity Sensor on a Silicon Multi-sensor chip for Fisheries Research

Hyldgård, Anders; Olafsdottir, Iris; Olesen, M.; Hedegaard, T.; Hansen, Ole; Thomsen, Erik Vilain

Published in:
Proceedings of IEEE sensors 2005

Link to article, DOI:
10.1109/ICSENS.2005.1597902

Publication date:
2005

Document Version
Publisher's PDF, also known as Version of record

FISH & CHIPS: Four Electrode Conductivity / Salinity Sensor on a Silicon Multi-sensor Chip for Fisheries Research

A. Hyldgård, Í. Ólafsdóttir, M. Olesen, T. Hedegaard, O. Hansen & E. V. Thomsen
Department of Micro and Nanotechnology (MIC)
Technical University of Denmark (DTU)
Kgs. Lyngby, Denmark
ahy@mic.dtu.dk

***Abstract*— The design and fabrication of a single chip silicon salinity, temperature, pressure and light multi-sensor is presented. The behavior 2- and 4-electrode conductivity micro-sensors is described, and methods for precise determination of water conductivity is given.**

I. INTRODUCTION

In recent time a significant focus has been set on fish behavior and fish population estimations due to the expected endangerment of certain species of fish mainly as a result of excessive fishing activity. Reliable monitoring of individual fish behavior and migration in their natural environment is crucial in order to make accurate population estimations and plans for preservation of the different species.

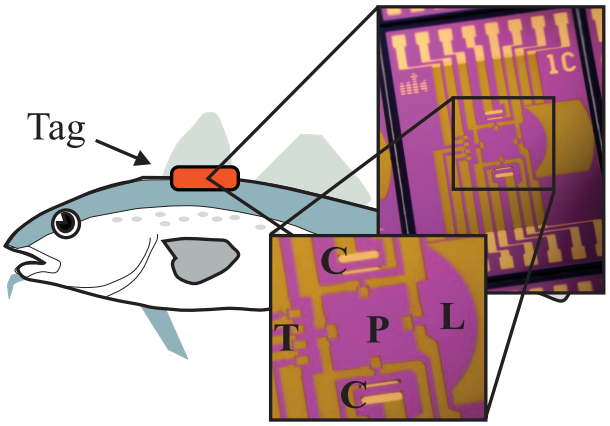

Figure 1. The sensor is placed on the back of a fish and is exposed directly to the seawater. On-board electronics stores the measured data. The sensor measures Temperature (T), Pressure (P), Light Intensity (L) and electrical conductivity (C).

A Data Storage Tag is an autonomous measurement system that, when sutured onto the back of a fish, can collect information about the fish surroundings. When the fish are re-caught the data can be retrieved. The salinity can be calculated from the conductivity, temperature and pressure triplet from well-established polynomial fits to empirical data [1]. Comparison with data of local variations can be used to estimate the local movement of the fish. The variation of light intensity during the day can be used to deduct the longitude and latitude. This information can be used to reconstruct fish migration and fish patterns of behavior [2]. Today, research on fish behavior is strongly limited by the considerable size of conventional discrete sensors. The aim is thus to make a microscale multi-sensor package that, when combined with suitable electronics and a compact packaging, will allow for a significantly smaller tag.

II. DESIGN

A multi-sensor (see Fig. 1) consisting of a piezoresistive Wheatstone bridge pressure sensor, a doped silicon thermistor, a pn-junction photodiode and a 4-electrode array, is arranged on the central 1.5x1.5mm^2 part of a 4x6mm^2 silicon chip. The contacts are placed on the ends of the chip and the sensors are contacted via a buried silicide layer in order to allow for direct exposure of the sensors to the water, while keeping the contacts dry. An O-ring packaging system is used to seal out the water [3].

III. FABRICATION

Fig. 2 shows a cross-sectional fabrication sequence for the multi-sensor chip. Different p-type resistors optimized for piezo resistivity, thermal sensitivity and high conductivity, are ion-implanted through a 100nm silicon dioxide layer into the single crystal n-type silicon (100) substrate. The resistive sensors have a resistance of approx.

This work is supported by *The Danish Institute for Fisheries Research http://www.dfu.min.dk*

0-7803-9056-3/05/$20.00 © 2005 IEEE.

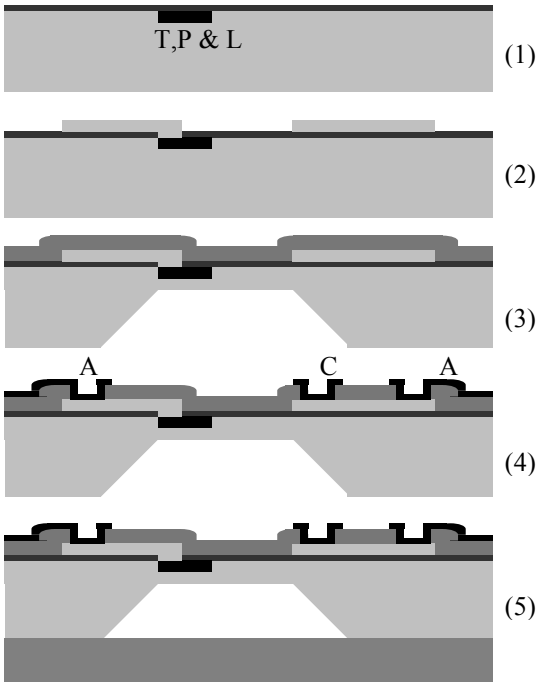

Figure 2. Chip fabrication sequence. (1) Sensors (T,P & L) are ion implanted. (2) $TiSi_2$ wiring is formed. (3) Si_3N_4 coating is deposited and a membrane is etched out. (4) Two metallizations form electrodes (C) and contact areas (A). (5) A Pyrex wafer is anodic bonded to the backside.

30kΩ to yield low power consumption while keeping a high signal to noise ratio.

The implanted resistors are contacted via a $TiSi_2$ wiring system made by RTP annealing of titanium and polysilicon at 800°C for 30s. The low sheet resistance of the 250nm $TiSi_2$ wiring ensures low parasitic series resistances between sensors and contacts even in long conductor paths ($R_{\square}$=1Ω).

Both sides of the wafer are coated with a 120nm LPCVD silicon nitride. The nitride is used as masking material in the subsequent KOH bulk silicon etch that forms the pressure sensor membrane. The backside nitride is then removed whereas the front-side nitride is kept as the protective coating of the sensors. Contact holes are made through the nitride by reactive ion etching in a SF_6/O_2 plasma.

The chips are metallized by platinum and gold to form electrodes and contact pads as the demands for corrosion inertness and wire bonding compatibility are not met by a single metal. The backside of the chip is anodic bonded to a Pyrex wafer to form a low-pressure reference cavity and add mechanical stability to the chip.

The complete process is only slightly more complex than processes used in commercial pressure sensor fabrication, and is well suited for batch processing.

IV. Results

Although the salinity is expressed by the conductivity, temperature and pressure triplet, it varies most with the conductivity [4]. A precise determination of conductivity is thus essential. Therefore the main focus is on the conductivity results.

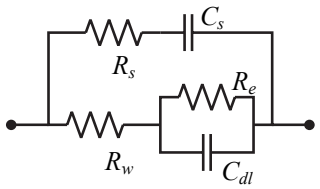

Figure 3. Conductance cell equivalent circuit. The electrolysis impedance R_e is much higher than the water impedance R_w. The double layer capacitance C_{dl} is higher than the parasitic capacitance C_s.

A. Conductivity

The electrical conductivity of the seawater is determined by measuring the impedance between 2 or 4 electrodes. Ideally the conductivity κ is related to the impedance Z through the relation $\kappa = K/Z$, where K is the geometrically determined cell constant. In reality, the relation is complicated by the presence of an electrochemical double layer capacitance (DLC) at the electrode-water interface and a parasitic conductance in the substrate. An equivalent model for the 2-electrode system is shown in Fig. 3 and the corresponding impedance can be expressed as

$$Z = \frac{1}{\dfrac{1}{R_w + \dfrac{1}{1/R_e + j\omega^{\alpha_1} C_{dl}}} + \dfrac{1}{R_s + \dfrac{1}{j\omega^{\alpha_2} C_s}}}.$$

For low frequencies the current is due to charge transfer by electrolysis. This gives an effectively high resistance R_e compared to the water resistance R_w. For medium frequencies the double layer capacitance C_{dl} starts conducting and changes in water conductivity due to changes in salinity can be observed.

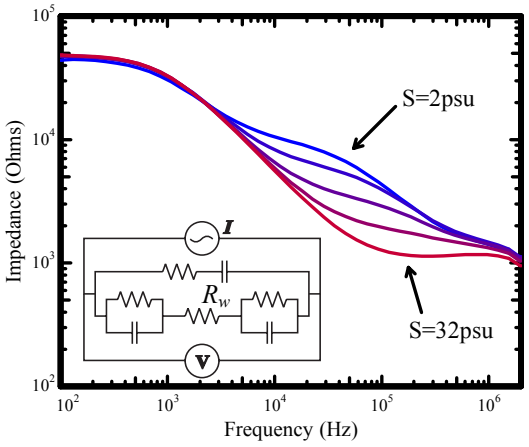

Figure 4. Impedance as a function of frequency for a 2-electrode cell at 5 different salinities (2, 4, 8, 16 and 32 psu). The double layer capacitance can be eliminated by extrapolation of the impedance to infinite frequency. Thus, the water resistance, R_w, can be determined.

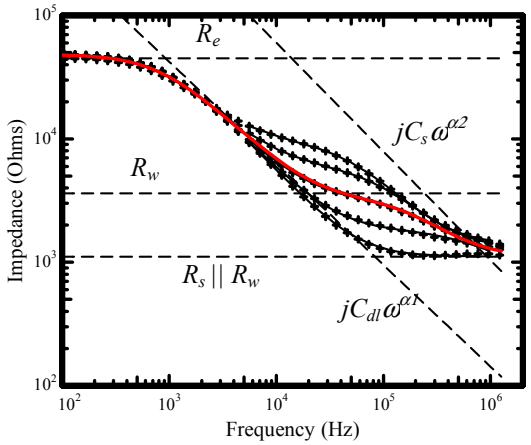

Figure 5. Model fit to the measured data. Dashed lines indicate the contributions to the complete fit indicated by the thick solid line.

Table 1. Parameters from model fit to measured data

Sal.	R_w (Ω)	R_e (Ω)	R_p (Ω)	C_{dl} (nF)	α_1	C_p (nF)	α_2
2	10517	50k	1.5k	289	0.68	5.2	0.91
4	6726	51k	1.7k	142	0.76	4.8	0.90
8	3618	49k	2.0k	80	0.82	4.5	0.89
16	1906	49k	3.1k	57	0.86	4.9	0.83
32	1116	49k	-	41	0.91	-	-

For high frequencies, the impedance is dominated by the parasitic conductance expressed by the substrate capacitance C_s and the substrate resistance R_s. Fig. 4 shows the impedance as a function of frequency measured with 2 electrodes at 5 different salinities. The model is fitted to the measured data as shown in Fig. 5 and the extracted parameters are presented in Table 1. The impedance behaves as expected and the slopes of the capacitances are numerically smaller than 1, which would be expected for normal capacitances.

For the DLC this is predicted in electrochemistry where the impedance is known to be proportional to $\omega^{-\alpha}$ where $\alpha < 1$. Both C_{dl} and α_1 changes with salinity which is in good agreement with the behavior of permanent and diffusive double layers. Fig. 6 shows the capacitances and the related power coefficients. For high salinities C_{dl} converges as the diffusive double layer becomes negligible. The slope of the parasitic transient can be explained by expanding the simple parasitic substrate capacitance with a distributed capacitance network as shown in Fig. 7. A simple distributed network has a typical frequency relation of $\omega^{-1/2}$. For that reason the more complex system at hand is modeled by $\omega^{-\alpha}$.

The extracted water conductance as a function of salinity is shown in Fig. 8. The almost linear relation is in good agreement with theory.

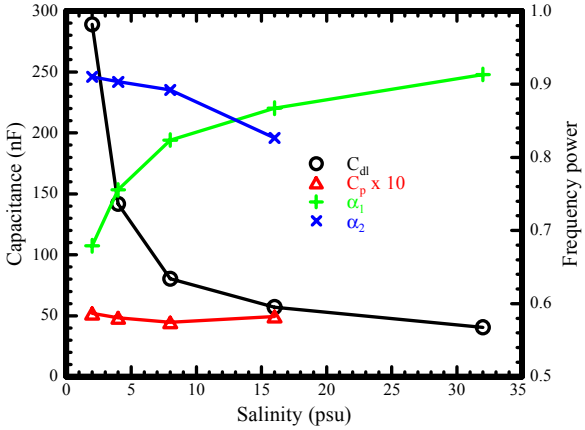

Figure 6. Model capacitances and the related power coefficients. For high salinities C_{dl} converges as the diffusive double layer becomes negligible.

In real applications, a simpler and more direct determination of the water conductivity is desirable. Determining the water conductivity directly from the impedance will introduce an error caused by the DLC. This can be eliminated by extrapolation to infinite frequency as described in [4]. Alternatively a 4-electrode configuration can be used. The transimpedance as a function of frequency for a 4-electrode cell is shown in Fig. 9. The DLC is not as evident at the measurement electrodes. However, a medium frequency AC current still has to run in the current electrodes in order to ensure a significant potential drop across the water.

For the simple 2-electrode and 4-electrode configuration there is a linear relation between the salinity and the water resistance extrapolated at a single frequency.

Fig. 10 shows the cell constant K and the standard deviation of the impedance/salinity linear fit as a function of frequency for the 2-electrode (extrapolated) and the 4-electrode configuration respectively.

Clearly the cell constant is higher for the 2-electrodes than for 4-electrodes. However, a higher impedance offset for the 2-electrode makes the difference in relative sensitivity less evident, as shown in Fig. 11. The peak in cell constant is also much wider and the 4-electrode configuration must be considered as being less sensitive to variations in frequency and DLC.

In order to optimize the conductivity cell the ratio between the upper and lower frequencies limiting the salinity window must be as high as possible, widening the frequency band in which impedance is strongly dependent of salinity.

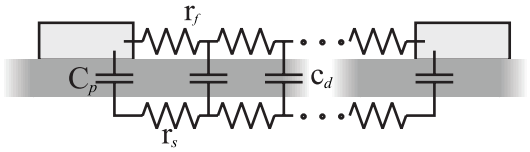

Figure 7. Distributed capacitance network. The dielectric film will serve as a capacitor stretching between the two electrodes. The impedance typically varies with $\omega^{-1/2}$. rf and cd represents the distributed parameters.

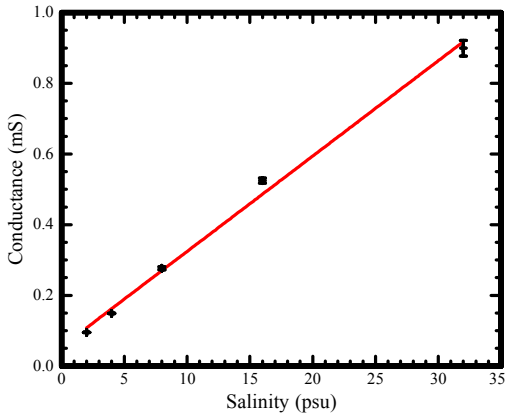

Figure 8. The inverse of the fitted water resistance as a function of salinity. The almost linear relation is in good agreement with theory.

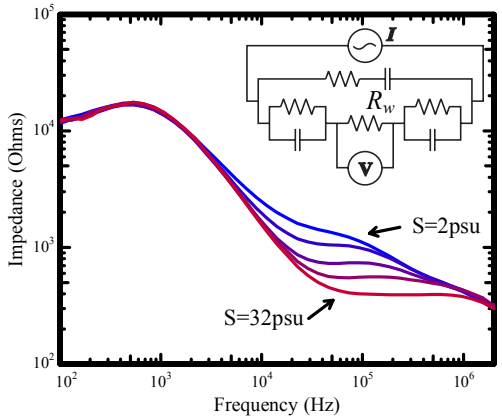

Figure 9. Transimpedance as a function of frequency for a 4-electrode cell at 5 different salinities (2, 4, 8, 16 and 32 psu). For medium to high frequencies the impedance is independent of the double layer when neglecting the parasitic impedance in the substrate.

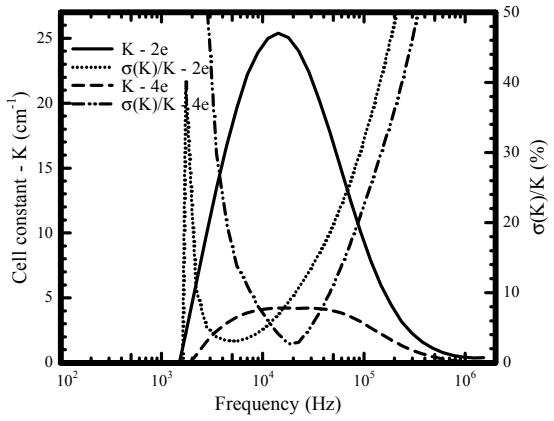

Figure 10. The 2-electrode and 4-electrode cell-constants as a function of frequency. σ represents the relative standard deviation of the cell constant as obtained from the linear regression. The 2-electrode has a high cell constant whereas the 4-electrode has a flat profile with *K* and σ peeks at the same frequency.

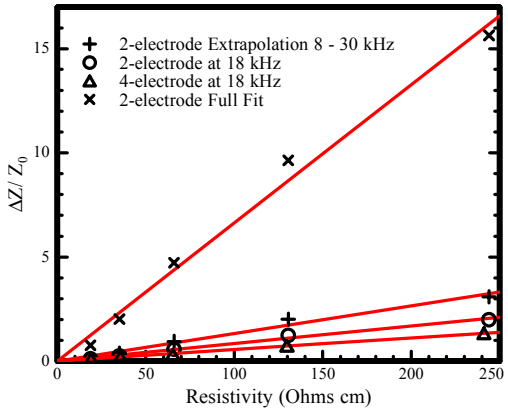

Figure 11. Relative change in cell impedance vs. saltwater resistivity. For simple extractions, the sensitivity (slope of fit) is higher for 2-electrode than for 4-electrode. 4-electrode signals are more stable for changes in electrode double layer capacitance. The optimum determination of water conductance comes from a complete fit.

Merely increasing the electrode area will not lower the low-end frequency as this will both increase the DLC and decrease *K*. Analytical approximations and FEM analysis indicates that thin long electrodes are the best solution for microsystems with limited electrode spacing. The high-end frequency scales with the inverse substrate capacitance. The capacitance can be lowered by limiting the area of the conducting paths, by increasing the dielectric thickness, and/or by increasing the substrate resistance.

B. Temperature and Light

The temperature sensor shows a high degree of linearity between thermistor resistance and reference temperature measured with a commercial PT100 element. There is no measurable time delay between the two temperature readings when submerged in liquid. The light sensor quantum efficiency (QE) is measured against a calibrated photodiode. The light sensor has a QE of 40-70% in the visible domain.

V. SUMMARY

The water conductivity and thereby the water salinity can be determined in different ways. A precise determination calls for a frequency scan whereas different methods allow for determination from few single frequencies. A wider frequency band can be obtained by changing the substrate capacitance.

REFERENCES

[1] E. L. Lewis, "The Practical Salinity Scale 1978 and its antecedents", IEEE Journal of Oceanic Engineering, 1980S.

[2] Neuenfeldt , H. Hinrichsen and A. Nielsen, "A method to geolocate eastern Baltic cod by using Data Storage Tags (DSTs)", ICES CM 2004/L:06

[3] C. Pedersen, S. T. Jespersen, K. W. Jacobsen, J. P. Krog, C. Christensen, and E. V. Thomsen, "Highly Reliable O-ring Packaging Concept for MEMS Pressure Sensors", Sensors and Actuators A 115 (2004) 617-627

[4] A. Hyldgård, O. Hansen, E.V. Thomsen, "Fish & Chips: Single Chip Silicon MEMS CTDL Salinity, Temperature, Pressure and Light Sensor for Use in Fisheries Research. IEEE MEMS 2005 proceedings, p. 303